Nanoscale

PAPER

View Article Online
View Journal | View Issue

Cite this: *Nanoscale*, 2024, **16**, 8013

Multi-stimuli-responsive polymer degradation by polyoxometalate photocatalysis and chloride ions†

Chen Gu,[a] Chifeng Li,[a] Noriyuki Minezawa,[b] Susumu Okazaki,*[b] Kazuya Yamaguchi[a] and Kosuke Suzuki*[a]

Received 26th January 2024,
Accepted 16th March 2024

DOI: 10.1039/d4nr00394b

rsc.li/nanoscale

Photocatalytic polymer degradation based on harnessing the abundant light energy present in the environment is one of the promising approaches to address the issue of plastic waste. In this study, we developed a multi-stimuli-responsive photocatalytic polymer degradation system facilitated by the photocatalysis of a polyoxometalate $[\gamma\text{-}PV_2W_{10}O_{40}]^{5-}$ in conjunction with chloride ions (Cl^-) as harmless and abundant stimuli. The degradation of various polymers was significantly accelerated in the presence of Cl^-, which was attributed to the oxidation of Cl^- by the polyoxometalate photocatalysis into a highly reactive chlorine radical that can efficiently generate a carbon-centered radical for subsequent polymer degradation. Although organic and organometallic photocatalysts decomposed under the conditions for photocatalytic polymer degradation in the presence of Cl^-, $[\gamma\text{-}PV_2W_{10}O_{40}]^{5-}$ retained its structure even under these highly oxidative conditions.

Introduction

Plastic waste has become a pressing environmental concern, demanding the development of effective technologies for polymer degradation.[1] Given that most plastics demonstrate stability and resist natural degradation processes in the environment, their improper disposal results in severe environmental harm. To address this issue, diverse waste management methods have been developed at both the fundamental research and industrial levels.[2] Among these, photocatalytic polymer degradation stands out as one of the promising techniques, as it is based on harnessing the readily available and abundant light energy from the environment without the need for specific polymer structures, excess amounts of reactants, and high reaction temperature.[3] Photocatalytic reactions truncate polymer chains and induce oxygenation, facilitating subsequent degradation by microorganisms. However, most photocatalytic systems rely solely on light as a stimulus and have difficulty in controlling the polymer degradation (Fig. 1a).

To achieve more controlled photocatalytic polymer degradation, we aimed to develop a photocatalytic system that requires multiple stimuli for polymer degradation beyond just light. The stimulus we focused on was chloride ions (Cl^-), which are innocuous and abundant in various salt forms in the environment and, more importantly, can be converted to highly reactive chlorine radicals ($Cl^{\bullet}$) *via* electrochemical or photochemical processes.[4,5] Photocleavage of the M–Cl bonds of chloride salts of various metals, such as Cu^{2+}, Fe^{3+}, Ni^{3+}, and Ti^{4+}, *via* ligand-to-metal charge transfer has been employed to generate $Cl^{\bullet}$.[6] In addition, since the one-electron

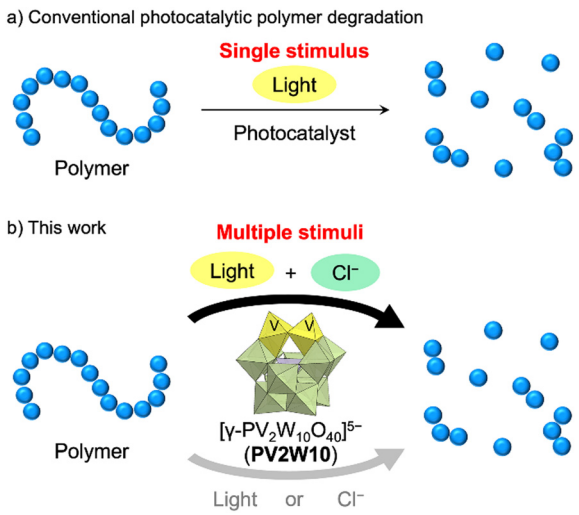

Fig. 1 Schematic representations of (a) a conventional photocatalytic polymer degradation system utilizing a single stimulus, light, and (b) this work: multi-stimuli-responsive polymer degradation by polyoxometalate photocatalysis utilizing both light and chloride ions.

[a]*Department of Applied Chemistry, School of Engineering, The University of Tokyo, Tokyo, Japan. E-mail: ksuzuki@appchem.t.u-tokyo.ac.jp*
[b]*Department of Applied Materials Science, Graduate School of Frontier Sciences, The University of Tokyo, Chiba, Japan. E-mail: okazaki@edu.k.u-tokyo.ac.jp*

† Electronic supplementary information (ESI) available. See DOI: https://doi.org/10.1039/d4nr00394b

oxidation potential of Cl^- is *ca.* +1.5 V *vs.* the normal hydrogen electrode,[7] photocatalytic oxidation processes with photoredox catalysts can also be harnessed to generate $Cl^\bullet$ from Cl^-.[4,8,9] Importantly, the generated $Cl^\bullet$ exhibits a remarkably high hydrogen atom transfer (HAT) ability, enabling it to abstract hydrogen atoms from various organic molecules, consequently generating carbon radicals. This propensity arises from the higher bond dissociation energy of H–Cl (103 kcal mol^{-1}) compared to that of typical H–C(sp^3) bonds (*e.g.*, H–CH_2CH_3, 101 kcal mol^{-1}; H–$CH(CH_3)_2$, 98.6 kcal mol^{-1}).[10] The carbon radicals generated *via* $Cl^\bullet$-mediated HAT can react with O_2, making this approach suitable for polymer degradation. While organic dye photocatalysts, like 9-mesityl-10-methylacridinium ion (Acr^+-Mes), have been reported to generate $Cl^\bullet$ from Cl^- by photo-irradiation,[8] they are susceptible to decomposition by $Cl^\bullet$ and are therefore unsuitable for polymer degradation.

Polyoxometalates (POMs) are anionic metal oxide clusters considered as emerging materials in the field of photocatalysts.[11,12] Their redox potentials and reactivities can be finely controlled by selecting their structures and constituent elements. In addition, POMs offer a distinct advantage as they have a significantly greater oxidative durability compared to organic dye and organometallic photocatalysts. We have recently reported a highly efficient polymer degradation system based on the photocatalysis of decatungstate $[W_{10}O_{32}]^{4-}$.[13] However, owing to its pronounced HAT ability, decatungstate photocatalysis for polymer degradation relies exclusively on photo-irradiation, without requiring additional stimuli. We have previously reported the visible-light-responsive photocatalysis of a vanadium-containing polyoxotungstate $[\gamma\text{-}PV_2W_{10}O_{40}]^{5-}$ (**PV2W10**, Fig. S1†) for the aerobic oxygenation of organic substrates *via* single electron transfer (SET) initiated by the photoactive catalyst.[14] In this study, by harnessing the photocatalytic SET property of **PV2W10**, we developed a system for multiple-stimuli-responsive polymer degradation that allows efficient degradation of various polymers when multiple stimuli, specifically, light and Cl^-, are present (Fig. 1b).

Results and discussion

We investigated the multi-stimuli-responsive photocatalytic degradation of polycaprolactone (PCL), our selected model polymer, using various photocatalysts, including POMs, organic dyes, organometallic complexes, and inorganic semiconductor photocatalysts. The PCL degradation experiments were conducted under photo-irradiation by a xenon lamp (λ > 350 nm) in acetonitrile with an O_2 atmosphere (1 atm) (Table 1, Fig. S2†). After 4 h of the photocatalytic reaction, the number-average and weight-average molecular weights of PCL (M_n and M_w) were determined *via* gel permeation chromatography. Degradation efficiency was evaluated based on the degradation rate, which was defined as $(M_{w0} - M_w)/M_{w0}$ (%) (where M_{w0} is M_w before reaction, Table 1, entry 1). PCL degradation by the tetra-*n*-butylammonium (TBA) salt of **PV2W10** ($TBA_4H[\gamma\text{-}PV_2W_{10}O_{40}]$, TBA**PV2W10**) hardly proceeded, resulting in a degradation rate of only 7% (Table 1, entry 2). In stark contrast, the addition of TBACl (tetra-*n*-butylammonium chloride) as a Cl^- source to the reaction solution significantly enhanced the degradation, achieving a degradation rate of 51% (Table 1, entry 3 and Fig. S3†). The degradation also proceeded when using visible light (λ > 400 nm, Table 1, entry 4). It is important to highlight that degradation did not proceed without photo-irradiation or under an argon (Ar) atmosphere (Table 1, entries 5 and 6). Furthermore, without TBA**PV2W10**, degradation did not proceed even when light, Cl^-, and O_2 were all present (Table 1, entry 7). These results firmly established that this multi-stimuli-responsive polymer degradation was realized by the photocatalysis of MgCl TBA**PV2W10**. Even when the amount of TBA**PV2W10** was reduced, the acceleration effect of Cl^- was still observed (Table S1†). Remarkably, this system was efficient also under sunlight. After 10 h of sunlight irradiation (Fig. S4†), the PCL degradation rates in the absence

Table 1 Photocatalytic PCL degradation by various catalysts in the presence or absence of Cl^-[a]

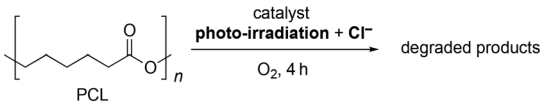

Entry	Catalyst	TBACl	M_w (kg mol^{-1})	$(M_{w0} - M_w)/M_{w0}$ (%)	M_w/M_n
1	(Before reaction)	—	20.8 (M_{w0})	—	1.72
2	TBA**PV2W10**	—	19.4	7	1.94
3	TBA**PV2W10**	Yes	10.2	51	1.89
4[a]	TBA**PV2W10**	Yes	10.8	48	1.95
5	TBA**PV2W10** (dark)	Yes	20.7	<1	1.78
6	TBA**PV2W10** (Ar)	Yes	22.0	<1	1.67
7	—	Yes	20.9	<1	1.76
8[b]	— (sunlight)	—	21.0	<1	1.72
9[c]	TBA**PV2W10** (sunlight)	—	18.5	11	1.80
10[c,d]	TBA**PV2W10** (sunlight)	Yes	14.6	30	1.81
11	TBA**W10**	—	3.98	81	1.53
12	TBA**W10**	Yes	7.40	64	2.17
13	$TBA_4H_2[\gamma\text{-}SiV_2W_{10}O_{40}]$	—	20.5	1	1.71
14	$TBA_4H_2[\gamma\text{-}SiV_2W_{10}O_{40}]$	Yes	17.8	15	1.88
15	$TBA_3[\alpha\text{-}PW_{12}O_{40}]$	—	19.6	6	1.75
16	$TBA_3[\alpha\text{-}PW_{12}O_{40}]$	Yes	19.4	7	1.75
17	$TBA_4[\alpha\text{-}PVW_{11}O_{40}]$	—	19.9	4	1.73
18	$TBA_4[\alpha\text{-}PVW_{11}O_{40}]$	Yes	19.8	5	1.75
19	$TBA_6[\alpha\text{-}PV_3W_9O_{40}]$	—	20.2	3	1.70
20	$TBA_6[\alpha\text{-}PV_3W_9O_{40}]$	Yes	20.0	4	1.74
21	Eosin Y	—	17.6	15	1.83
22	Eosin Y	Yes	14.9	29	1.92
23	Acr^+-Mes ClO_4^-	—	19.6	6	1.80
24	Acr^+-Mes ClO_4^-	Yes	16.3	22	1.94
25	$Ru(bpy)_3Cl_2$	—	19.8	5	1.78
26	$Ru(bpy)_3Cl_2$	Yes	19.6	6	1.83
27[e]	TiO_2 (ST-01)	—	18.1	13	2.35
28[e]	TiO_2 (ST-01)	Yes	18.4	11	1.87

Reaction conditions: PCL (40 mg), catalyst (0.0011 mmol, equivalent to 4 mg of TBA**PV2W10**), TBACl (4 mg), O_2 (1 atm), acetonitrile (4 mL), photo-irradiation (xenon lamp, λ > 350 nm), 4 h. After the reaction, M_w and M_n were determined by gel permeation chromatography. [a] Photo-irradiation (xenon lamp, λ > 400 nm). [b] Sunlight 10 h. [c] Sunlight 10 h, TBA**PV2W10** (9 mg). [d] TBACl (8 mg). [e] TiO_2 (4 mg).

and presence of TBA**PV2W10** were only <1% and 11%, respectively (Table 1, entries 8 and 9). On the other hand, the coexistence of TBA**PV2W10** and Cl^- significantly accelerated PCL degradation, leading to a degradation rate of 30% (Table 1, entry 10).

We also explored the utility of other photocatalysts. As we recently reported, TBA**W10**, the TBA salt of decatungstate ($TBA_4[W_{10}O_{32}]$) is an exceptionally reactive photocatalyst for polymer degradation.[13] With TBA**W10**, PCL degradation proceeded both in the absence and presence of Cl^-, and multi-stimuli-responsive polymer degradation could not be achieved (Table 1, entries 11 and 12). $TBA_4H_2[\gamma\text{-}SiV_2W_{10}O_{40}]$, which has the same structure as TBA**PV2W10** but contains different heteroatoms (Si and P), also exhibited enhanced reactivity for PCL degradation when Cl^- was present (Table 1, entries 13 and 14). However, the enhancement was much lower than that obtained with TBA**PV2W10**, resulting in a degradation rate of only 15% even in the presence of Cl^- (Table 1, entry 14). In contrast, $TBA_3[\alpha\text{-}PW_{12}O_{40}]$, $TBA_4[\alpha\text{-}PVW_{11}O_{40}]$, and $TBA_6[\alpha\text{-}PV_3W_9O_{40}]$ hardly showed any activity for PCL degradation under photo-irradiation (Table 1, entries 15–20).

Organic dye photocatalysts, such as Eosin Y and Acr^+-Mes ClO_4^-, proved ineffective in this system (Table 1, entries 21–24). Although Eosin Y is known to promote various reactions *via* both SET and HAT processes,[15] the UV-Vis spectra revealed its decomposition during PCL degradation under photo-irradiation (Fig. 2a and b).[16] In addition, previous reports have shown that Acr^+-Mes ClO_4^- can generate $Cl^\bullet$ from Cl^- *via* photo-irradiation;[8] however, reactivity for PCL degradation remained modest, achieving a degradation rate of only 22% in the presence of Cl^- (Table 1, entries 23 and 24). Notably, although Acr^+-Mes ClO_4^- is stable under photo-irradiation in the absence of Cl^- (Fig. 2c), the absorbance of Acr^+-Mes ClO_4^- in the UV-Vis spectrum significantly decreased under photo-irradiation in the presence of Cl^-, revealing an issue with its durability (Fig. 2d). This was likely caused by the decomposition of Acr-Mes^+ ClO_4^- by the highly reactive $Cl^\bullet$ generated from Cl^-. In contrast, TBA**PV2W10** can maintain its structure even under oxidative conditions. The UV-Vis and ^{31}P and ^{51}V NMR spectra proved that the structure of TBA**PV2W10** was maintained even after polymer degradation in the presence of Cl^- (Fig. 2e–h). Slight changes in the absorbance of the UV-Vis spectrum and ^{31}P NMR chemical shifts were likely attributed to TBA**PV2W10** protonation during the reaction rather than decomposition of the catalyst (Fig. S5–S7†). The durable TBA**PV2W10** provided superior catalytic activity compared to these organic dyes. The organometallic photocatalyst $Ru(bpy)_3Cl_2$ was not effective for polymer degradation, either in the absence or presence of Cl^- (Table 1, entries 25 and 26). This was likely due to its structural change, as observed in the UV-Vis spectra (Fig. S8†). These results revealed that organic and organometallic photocatalysts have durability issues under the conditions of polymer degradation where various reactive radical species, including $Cl^\bullet$, are generated. TiO_2, a well-studied photocatalyst for polymer degradation,[3] was also assessed. Although TiO_2 showed low efficiency in polymer degradation (degradation rate, 13%) without Cl^- by photo-irradiation, it did not exhibit multi-stimuli-responsive polymer degradation in the presence of Cl^- (Table 1, entries 27 and 28).

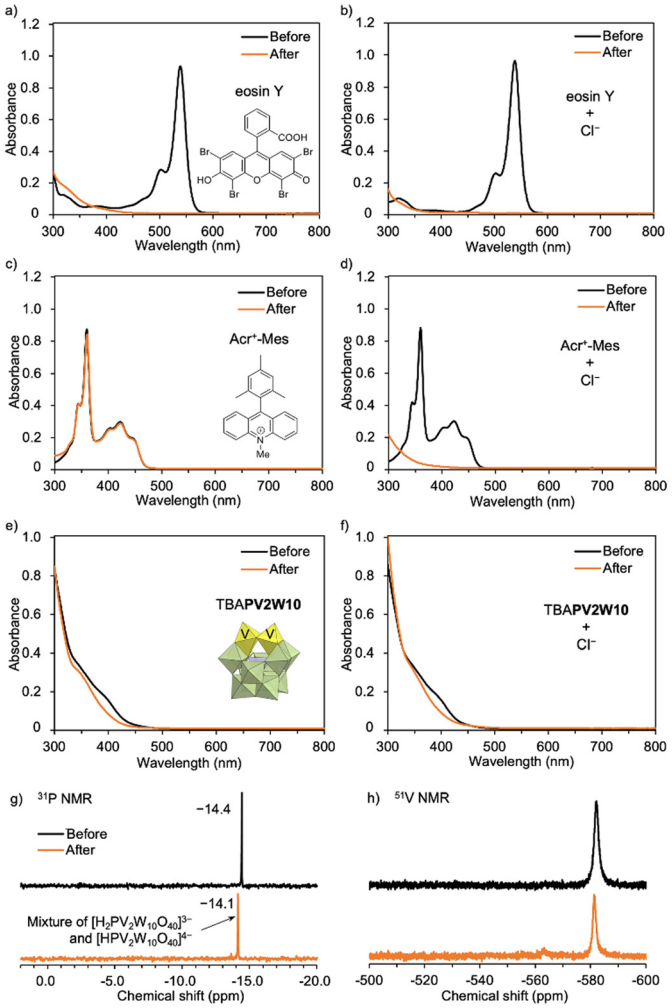

Fig. 2 Stability test for various photocatalysts. UV-vis spectra of (a and b) Eosin Y, (c and d) Acr^+-Mes ClO_4^-, (e and f) TBA**PV2W10** before and after PCL degradation in the absence and presence of Cl^- by photo-irradiation (λ > 350 nm) for 4 h. (g) ^{31}P and (h) ^{51}V NMR spectra of TBA**PV2W10** before and after PCL degradation in the presence of Cl^- by photo-irradiation (λ > 350 nm) for 4 h.

Next, we investigated the effect of Cl^- by employing various counter cations of Cl^- and other anions as additives while using TBA**PV2W10** as a photocatalyst (Table 2). When tetramethylammonium (TMA), tetrabutylphosphonium (TBP), and tetraphenylphosphonium (TPP) were employed as counter cations instead of TBA, they exhibited a comparable PCL degradation activity (in terms of degradation rate) to that under the system employing TBACl (Table 2, entries 1–6). This indicated that the choice of counter cation did not have any noticeable effect on this system. Furthermore, the inorganic salts LiCl and NaCl also accelerated PCL degradation under TBA**PV2W10** photocatalysis, despite their incomplete dissolution in the solution (Table 2, entries 7 and 8). In contrast, when bromide

Table 2 Photocatalytic PCL degradation by TBA**PV2W10** in the presence of various additives

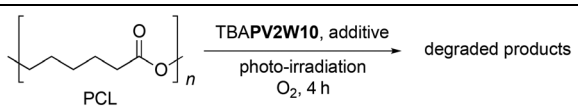

Entry	Additive	M_w (kg mol^{-1})	$(M_{w0} - M_w)/M_{w0}$ (%)	M_w/M_n
1	(Before reaction)	20.8 (M_{w0})	—	1.72
2	—	19.4	7	1.94
3	TBACl	10.2	51	1.89
4	TMACl	8.65	58	1.92
5	TBPCl	8.82	58	1.97
6	TPPCl	9.16	56	1.90
7	LiCl	11.4	45	2.06
8	NaCl	16.4	21	2.00
9	TBABr	16.5	21	1.86
10	TBPBr	15.1	27	1.80
11	TPPBr	15.0	28	1.82
12	TBAI	20.0	4	1.73
13	$TBAHSO_4$	16.7	20	2.04

Reaction conditions: PCL (40 mg), TBA**PV2W10** (4 mg), additive (0.014 mmol), O_2 (1 atm), acetonitrile (4 mL), photo-irradiation (λ > 350 nm), 4 h.

(Br^-), iodide (I^-), and hydrogen sulfate (HSO_4^-) ions were employed instead of Cl^-, the degradation rates significantly changed depending on the type of anion used (Table 2, entries 9–13 *vs.* entries 3–6). While Br^- and HSO_4^- showed PCL degradation capabilities *via* TBA**PV2W10** photocatalysis, the degradation rates were significantly lower than when Cl^- was employed. When TBAI was employed, the degradation hardly proceeded (Table 2, entry 12). Interestingly, the PCL degradation rates decreased in the order of TBACl > TBABr > TBAI, aligning with the order of the electron detachment energies of halogen anions (X^-),[17] the order of the bond dissociation energies of H–X (X = Cl, Br, and I), and the HAT ability of the corresponding halogen radicals ($X^•$).[10] These results indicated that this photocatalytic degradation system proceeded *via* oxidation of X^- to the corresponding radicals by TBA**PV2W10** photocatalysis, followed by halogen-radical-mediated HAT, resulting in the generation of carbon radicals on the polymer.

To investigate this hypothesis, we conducted the reaction in the presence of 2,2,6,6-tetramethylpiperidine 1-oxyl (TEMPO) or 2,6-di-*tert*-butyl-*p*-cresol (BHT), which are commonly used radical scavengers. When TEMPO was added to the reaction, the degradation rate decreased from 51% to 24% (Table S2,† entries 2 and 3). Similarly, the addition of BHT also led to a decrease in the degradation rate (Table S2,† entries 2 and 4). PCL degradation was inhibited by radical scavengers, suggesting that the process is regulated by a radical-mediated mechanism. In particular, TEMPO showed a greater suppression than BHT, suggesting that degradation proceed with the generation of carbon radicals followed by oxygen insertion.[18,19] The ^{1}H NMR spectrum of PCL after photocatalytic degradation by TBA**PV2W10** in the presence of Cl^- showed the formation of formate esters and aldehydes, which derived from oxidative chain cleavage (Fig. S9†).

To confirm the generation of $Cl^•$ during the photocatalytic reaction, we applied photo-irradiation to an acetonitrile solution containing TBA**PV2W10**, Cl^-, and styrene in an O_2 atmosphere. The subsequent GC-mass analysis of the solution confirmed the production of phenacyl chloride along with other oxidation products (Fig. S10 and S11†). Phenacyl chloride likely formed through the addition of $Cl^•$ to the C=C bond of styrene, followed by the introduction of O_2 at the benzyl position.[20] These results supported the conversion of Cl^- to $Cl^•$ by the TBA**PV2W10** photocatalysis.

Density functional theory calculations were employed to delve deeper into the mechanism of this system. First, the reactivity of the photo-excited **PV2W10** with Cl^- was evaluated. The spin density distribution of the lowest triplet state of the **PV2W10**–Cl^- complex showed that one of the unpaired electrons was located at the Cl atom, indicating that SET occurred from the photocatalyst to the Cl atom, resulting in **PV2W10**$^{•-}$–$Cl^•$ (Fig. S12†). Thermodynamic calculations also confirmed the experimental results. As shown in Table S3,† the one-electron oxidation of Cl^- by the lowest triplet state of **PV2W10** was exergonic. The Gibbs free energy of the reaction for **PV2W10** (T_1) + Cl^- → **PV2W10**$^-$ + $Cl^•$ was negative (−18.3 kcal mol^{-1}), revealing that this electron transfer was thermodynamically favorable. Importantly, the one-electron oxidation by the ground state **PV2W10** was 42.3 kcal mol^{-1} weaker than in the excited state, and the electron abstraction from Cl^- was thermodynamically unfavorable (+23.9 kcal mol^{-1}). These results indicated that $Cl^•$ may have formed through the oxidation of Cl^- by the photo-excited **PV2W10** rather than the ground-state one. Furthermore, we confirmed that $Cl^•$ can abstract a hydrogen atom from PCL to produce a carbon-centered radical. The Gibbs free energy of the reaction for abstraction of a hydrogen atom from model PCL using $Cl^•$ ranged from −11 to −17 kcal mol^{-1} (Table S4†). Moreover, the calculations corresponded to the order of the PCL degradation rates: Cl^- > Br^- > I^- (Table 2). Both the electron detachment energy[17] and the Gibbs free energy of the reaction (Table S3†) indicated that the heavier halide ion was more easily oxidized, but the reactivity of the formed radicals reversed (Table S4†). In particular, the iodine-mediated HAT reactions were highly endergonic in all cases, which is consistent with the experimental results showing essentially no degradation reaction.

Based on these findings, we propose a plausible mechanism regulating this multi-stimuli-responsive polymer degradation (Fig. 3). Cl^- was oxidized by photo-exited **PV2W10** to form $Cl^•$, which performed HAT on the polymer to generate a carbon radical, followed by oxidative chain cleavage.

Finally, we investigated the applicability of the multi-stimuli-responsive polymer degradation system to various polymers (Fig. 4 and Table S4†). In addition to degrading PCL, this system can efficiently degrade various other polymers, such as poly(1,4-butylene adipate) (PBA), polyvinyl acetate (PVAC), and cellulose acetate (CA), by photo-irradiation in the presence of both TBA**PV2W10** and Cl^-. In particular, the degradation rate of these polymers was significantly enhanced in the presence of Cl^-. In contrast, polyethers with low bond dissociation ener-

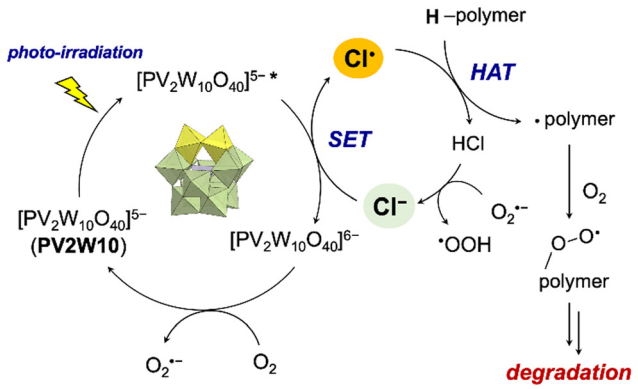

Fig. 3 Proposed mechanism regulating multi-stimuli-responsive polymer degradation by TBA**PV2W10** and Cl^-.

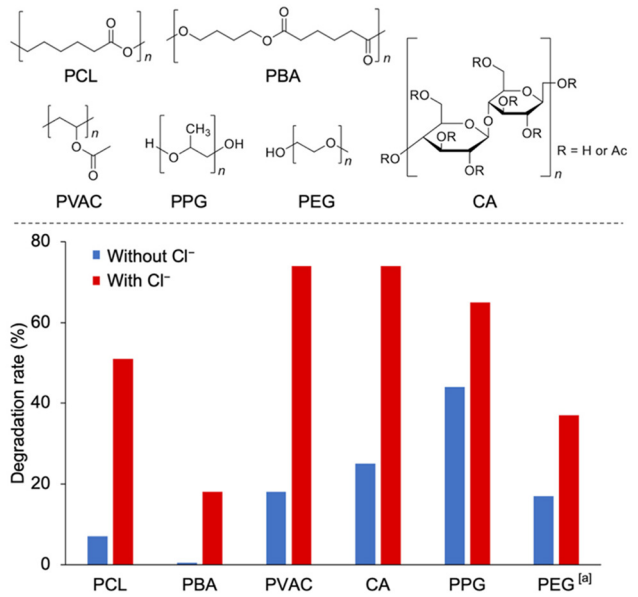

Fig. 4 Photocatalytic degradation of various polymers by TBA**PV2W10** in the absence and presence of Cl^-. Reaction conditions: polymer (40 mg), TBA**PV2W10** (4 mg), TBACl (4 mg), O_2 (1 atm), acetonitrile (4 mL), photo-irradiation (λ > 350 nm), 4 h. [a] Cs**PV2W10** (1.8 mg), NaCl (0.42 mg), water (4 mL), 2 h.

gies and low redox potentials, such as poly(propylene glycol) (PPG), underwent degradation *via* TBA**PV2W10** photocatalysis, with moderate enhancement of the degradation rate in the presence of Cl^-. The system was also shown to degrade polymers in water by using a water-soluble Cs salt of **PV2W10** ($Cs_5[\gamma\text{-}PV_2W_{10}O_{40}]$, Cs**PV2W10**). By employing the photocatalysis of Cs**PV2W10**, polyethylene glycol (PEG) degradation was facilitated in the presence of NaCl in water.

The results revealed a good correlation between the degradation rate of the polymers and their redox properties. Table S3† shows that the Gibbs free energy of the reaction for polyethers (PPG and PEG) was comparable to that of Cl^-. Thus, a direct electron transfer from the polymer to the photocatalyst is a plausible mechanism that works similarly in the absence of Cl^- ions, and such a mechanism is consistent with the experiment (Fig. 4), showing that polyethers can degrade quickly even without Cl^-. The carbon radical cations generated by the transfer of electrons to the photocatalyst may also cause fragmentation. The enhancement of polymer degradation by Cl^- may be due to an increase in ion-derived radical initiators. In contrast, the SET reaction of polyesters (PCL and PBA) and PVAC was slightly endergonic, and the SET mechanism leading to the formation of carbon radical cations was less favorable (Table S3†). Furthermore, the HAT by $Cl^\bullet$ provided an exergonic reaction pathway to the polymer's radical species (Table S4†).

Conclusions

In conclusion, we developed a photocatalytic polymer degradation system that requires multiple stimuli. This system harnesses the photoredox property of a polyoxometalate, $TBA_4H[\gamma\text{-}PV_2W_{10}O_{40}]$ (TBA**PV2W10**), requiring both light and chloride ions (Cl^-) as stimuli. In the presence of Cl^-, the degradation rate of PCL, defined as $(M_{w0} - M_w)/M_{w0}$ (%) (where M_{w0} is M_w before reaction), using TBA**PV2W10** under photo-irradiation was significantly enhanced (degradation rate 7% without Cl^-, 51% with Cl^-). This enhancement was attributed to the oxidation of Cl^- to highly reactive chlorine radical ($Cl^\bullet$) by the photo-activated TBA**PV2W10**. The $Cl^\bullet$ species exhibited a notable ability to transfer hydrogen atoms, allowing their abstraction from polymers to generate carbon-centered radicals for subsequent polymer degradation. Although organic and organometallic photocatalysts significantly decomposed under the conditions of photocatalytic polymer degradation in the presence of Cl^-, TBA**PV2W10** retained its structure even under these highly oxidative conditions. Moreover, this multi-stimuli-responsive polymer degradation system demonstrated its effectiveness across various types of polymer and was capable of operating even under sunlight and in water. We believe that this system will open new possibilities for the development of polymer degradation methods in environments where Cl^- and light can be harnessed, such as the ocean.

Conflicts of interest

There are no conflicts of interest to declare.

Acknowledgements

We gratefully acknowledge financial support from the New Energy and Industrial Technology Development Organization (NEDO), JST FOREST (JPMJFR213M), JSPS KAKENHI (22H04971), and the JSPS Core-to-Core program. We thank Prof. K. Ito and Dr S. Ando (The University of Tokyo) for their help in polymer analysis and fruitful discussion.

References

1 (*a*) D. K. A. Barnes, F. Galgani, R. C. Thompson and M. Barlaz, *Philos. Trans. R. Soc. London, Ser. B*, 2009, **364**, 1985–1998; (*b*) J. R. Jambeck, R. Geyer, C. Wilcox, T. R. Siegler, M. Perryman, A. Andrady, R. Narayan and K. L. Law, *Science*, 2015, **347**, 768–771; (*c*) R. Geyer, J. R. Jambeck and K. L. Law, *Sci. Adv.*, 2017, **3**, e1700782; (*d*) M. MacLeod, H. P. H. Arp, M. B. Tekman and A. Jahnke, *Science*, 2021, **373**, 61–65; (*e*) A. Chamas, H. Moon, J. Zheng, Y. Qiu, T. Tabassum, J. H. Jang, M. Abu-Omar, S. L. Scott and S. Suh, *ACS Sustainable Chem. Eng.*, 2020, **8**, 3494–3511; (*f*) A. Cózar, F. Echevarria, J. I. González-Gordillo, X. Irigoien, B. Úbeda, S. Hernández-León, A. T. Palma, S. Navarro, J. García-de-Lomas, A. Ruiz, M. L. Fernández-de-Puelles and C. M. Duarte, *Proc. Natl. Acad. Sci. U. S. A.*, 2014, **111**, 10239–10244.

2 (*a*) J. Hopewell, R. Dvorak and E. Kosior, *Philos. Trans. R. Soc. London, Ser. B*, 2009, **364**, 2115–2126; (*b*) S. C. Kosloski-Oh, Z. A. Wood, Y. Manjarrez, J. P. de los Rios and M. E. Fieser, *Mater. Horiz.*, 2021, **8**, 1084–1129; (*c*) I. Vollmer, M. J. F. Jenks, M. C. P. Roelands, R. J. White, R. J. White, T. van Harmelen, P. de Wild, G. P. Van der Laan, F. Meirer, J. T. F. Keurentjes and B. M. Weckhuysen, *Angew. Chem., Int. Ed.*, 2020, **59**, 15402–15423; (*d*) T. P. Haider, C. Völker, J. Kramm, K. Landfester and F. R. Wurm, *Angew. Chem., Int. Ed.*, 2019, **58**, 50–62; (*e*) M. S. Qureshi, A. Oasmaa, H. Pihkola, I. Deviatkin, A. Tenhunen, J. Mannila, H. Minkkinen, M. Pohjakallio and J. Laine-Ylijoki, *J. Anal. Appl. Pyrolysis*, 2020, **152**, 104804; (*f*) A. Rahimi and J. M. García, *Nat. Rev. Chem.*, 2017, **1**, 0046; (*g*) J. Zhou, T. G. Hsu and J. Wang, *Angew. Chem., Int. Ed.*, 2023, **62**, e202300768; (*h*) R. Miandad, M. A. Barakat, A. S. Aburiazaiza, M. Rehan and A. S. Nizami, *Process Saf. Environ. Prot.*, 2016, **102**, 822–838.

3 (*a*) W. Li, W. Zhao, H. Zhu, Z. J. Li and W. Wang, *J. Mater. Chem. A*, 2023, **11**, 2503–2527; (*b*) Z. Ouyang, Y. Yang, C. Zhang, S. Zhu, L. Qin, W. Wang, D. He, Y. Zhou, H. Luo and F. Qin, *J. Mater. Chem. A*, 2021, **9**, 13402–13441; (*c*) I. Nabi, A. U. R. Bacha, F. Ahmad and L. Zhang, *J. Environ. Chem. Eng.*, 2021, **9**, 105964; (*d*) P. Ebrahimbabaie, K. Yousefi and J. Pichtel, *Sci. Total Environ.*, 2022, **806**, 150603; (*e*) S. Chu, B. Zhang, X. Zhao, H. S. Soo, F. Wang, R. Xiao and H. Zhang, *Adv. Energy Mater.*, 2022, **12**, 2200435.

4 N. Fu, G. S. Sauer and S. Lin, *J. Am. Chem. Soc.*, 2017, **139**, 15548–15553.

5 (*a*) Y. Itabashi, H. Asahara and K. Ohkubo, *Chem. Commun.*, 2023, **59**, 7506–7517; (*b*) S. Bonciolini, T. Noël and L. Capaldo, *Eur. J. Org. Chem.*, 2022, e202200417.

6 (*a*) J. K. Kochi, *J. Am. Chem. Soc.*, 1962, **84**, 2121–2127; (*b*) Y. Abderrazak, A. Bhattacharyya and O. Reiser, *Angew. Chem., Int. Ed.*, 2021, **60**, 21100–21115; (*c*) F. Juliá, *ChemCatChem*, 2022, **14**, e202200916; (*d*) B. J. Shields and A. G. Doyle, *J. Am. Chem. Soc.*, 2016, **138**, 12719–12722; (*e*) S. M. Treacy and T. Rovis, *J. Am. Chem. Soc.*, 2021, **143**, 2729–2735; (*f*) Y. C. Kang, S. M. Treacy and T. Rovis, *ACS Catal.*, 2021, **11**, 7442–7449; (*g*) S. Oh and E. E. Stache, *J. Am. Chem. Soc.*, 2022, **144**, 5745–5749.

7 (*a*) R. Bevernaegie, S. A. M. Wehlin, E. J. Piechota, M. Abraham, C. Philouze, G. J. Meyer, B. Elias and L. Troian-Gautier, *J. Am. Chem. Soc.*, 2020, **142**, 2732; (*b*) A. M. Deetz, L. Troian-Gautier, S. A. M. Wehlin, E. J. Piechota and G. J. Meyer, *J. Phys. Chem. A*, 2021, **125**, 9355.

8 (*a*) K. Ohkubo, A. Fujimoto and S. Fukuzumi, *Chem. Commun.*, 2011, **47**, 8515–8517; (*b*) H. P. Deng, Q. Zhou and J. Wu, *Angew. Chem., Int. Ed.*, 2018, **57**, 12661–11284.

9 (*a*) S. Rohe, A. O. Morris, T. McCallum and L. Barriault, *Angew. Chem., Int. Ed.*, 2018, **57**, 15664–15669; (*b*) M. Zidan, A. O. Morris, T. McCallum and L. Barriault, *Eur. J. Org. Chem.*, 2020, 1453–1458; (*c*) C. Y. Huang, J. Li and C. J. Li, *Nat. Commun.*, 2021, **12**, 4010.

10 S. J. Blanksby and G. B. Ellison, *Acc. Chem. Res.*, 2003, **36**, 255–263.

11 (*a*) M. T. Pope, *Heteropoly and Isopoly Oxometalates*, Springer, Berlin, 1983; (*b*) C. L. Hill and C. M. Prosser-McCartha, *Coord. Chem. Rev.*, 1995, **143**, 407–455; (*c*) N. Mizuno and M. Misono, *Chem. Rev.*, 1998, **98**, 199–218; (*d*) R. Neumann, *Prog. Inorg. Chem.*, 1998, **47**, 317; (*e*) D. L. Long, R. Tsunashima and L. Cronin, *Angew. Chem., Int. Ed.*, 2010, **49**, 1736–1758; (*f*) S. S. Wang and G. Y. Yang, *Chem. Rev.*, 2015, **115**, 4893–4962; (*g*) A. Misra, K. Kozma, C. Streb and M. Nyman, *Angew. Chem., Int. Ed.*, 2020, **59**, 596–612; (*h*) J. M. Cameron, G. Guillemot, T. Galambos, S. S. Amin, E. Hampson, K. M. Haidaraly, G. N. Newton and G. Izzet, *Chem. Soc. Rev.*, 2022, **51**, 293–328; (*i*) K. Yonesato, D. Yanai, S. Yamazoe, D. Yokogawa, T. Kikuchi, K. Yamaguchi and K. Suzuki, *Nat. Chem.*, 2023, **15**, 940–947; (*j*) N. Ogiwara and S. Uchida, *Chem Catal.*, 2023, **3**, 100607.

12 (*a*) K. Suzuki, N. Mizuno and K. Yamaguchi, *ACS Catal.*, 2018, **8**, 10809–10825; (*b*) C. Streb, *Dalton Trans.*, 2012, **41**, 1651–1659; (*c*) H. Lv, Y. V. Geletii, C. Zhao, J. W. Vickers, G. Zhu, Z. Luo, J. Song, T. Lian, D. G. Musaev and C. L. Hill, *Chem. Soc. Rev.*, 2012, **41**, 7572–7589; (*d*) J. Lan, Y. Wang, B. Huang, Z. Xiao and P. Wu, *Nanoscale Adv.*, 2021, **3**, 4646–4658; (*e*) X. Chen, H. Wu, X. Shi and L. Wu, *Nanoscale*, 2023, **15**, 9242–9255.

13 (*a*) C. Li, C. Gu, K. Yamaguchi and K. Suzuki, *Nanoscale*, 2023, **15**, 15038–15042; (*b*) N. Minezawa, K. Suzuki and S. Okazaki, *Phys. Chem. Chem. Phys.*, DOI: **10.1039/D4CP00362D**.

14 C. Li, K. Suzuki, N. Mizuno and K. Yamaguchi, *Chem. Commun.*, 2018, **54**, 7127–7130.

15 (*a*) D. P. Hari and B. König, *Chem. Commun.*, 2014, **50**, 6688–6699; (*b*) X. Z. Fan, J. W. Rong, H. Wu, Q. Zhou, H. P. Deng, J. D. Tan, C. W. Xue, L. Z. Wu, H. Tao and J. Wu, *Angew. Chem., Int. Ed.*, 2018, **57**, 8514–8518; (*c*) D. M. Yan, J. R. Chen and W. J. Xiao, *Angew. Chem., Int. Ed.*, 2019, **58**, 378–380.

16 A. Alvarez-Martin, S. Trashin, M. Cuykx, A. Covaci, K. De. Wael and K. Janssens, *Dyes Pigm.*, 2017, **145**, 376–384.
17 B. Winter, R. Weber, I. V. Hertel, M. Faubel, P. Jungwirth, E. C. Brown and S. E. Bradforth, *J. Am. Chem. Soc.*, 2005, **127**, 7203–7214.
18 T. Vogler and A. Studer, *Synthesis*, 2008, 1979–1993.
19 W. A. Yehye, N. A. Rahman, A. Ariffin, S. B. A. Hamid, A. A. Alhadi, F. A. Kadir and M. Yaeghoobi, *Eur. J. Med. Chem.*, 2015, **101**, 295–312.
20 S. Tian, X. Jia, L. Wang, B. Li, S. Liu, L. Ma, W. Gao, Y. Wei and J. Chen, *Chem. Commun.*, 2019, **55**, 12104–12107.